



Published in final edited form as:

*Crit Care Med.* 2022 June 01; 50(6): e504–e515. doi:10.1097/CCM.0000000000005437.

## Drp1/Fis1-Dependent Pathologic Fission and Associated Damaged Extracellular Mitochondria Contribute to Macrophage Dysfunction in Endotoxin Tolerance

Riddhita Mukherjee, PhD<sup>1,2</sup>, Carly M. Tompkins, BS<sup>1,2</sup>, Nicolai Patrick Ostberg, BS<sup>2</sup>, Amit U. Joshi, PhD<sup>2</sup>, Liliana M. Massis, PhD<sup>3</sup>, Vijith Vijayan, PhD<sup>1</sup>, Kanika Gera, PhD<sup>1</sup>, Denise Monack, PhD<sup>3</sup>, Timothy T. Cornell, MD<sup>1</sup>, Mark W. Hall, MD<sup>4</sup>, Daria Mochly-Rosen, PhD<sup>2</sup>, Bereketeab Haileselassie, MD<sup>1,2</sup>

<sup>1</sup>Department of Pediatrics, Division of Critical Care Medicine, Stanford University School of Medicine, Stanford, CA, 94305; USA

<sup>2</sup>Department of Chemical and Systems Biology, Stanford University School of Medicine, Stanford, CA, 94305; USA

<sup>3</sup>Department of Microbiology and Immunology, Stanford University School of Medicine, Stanford, CA, 94305; USA

<sup>4</sup>Department of Pediatrics, Division of Critical Care Medicine, Nationwide Children's Hospital, Columbus, OH, 43205; USA

### Abstract

**Objective:** Recent publications have shown that mitochondrial dynamics can govern the quality and quantity of extracellular mitochondria subsequently impacting immune phenotypes. This study aims to determine if pathologic mitochondrial fission mediated by Drp1/Fis1 interaction impacts extracellular mitochondrial content and macrophage function in sepsis-induced immunoparalysis.

**Design:** Laboratory investigation.

**Setting:** University laboratory.

**Interventions:** Using *in vitro* and murine models of endotoxin tolerance, we evaluated changes in Drp1/Fis1-dependent pathologic fission and simultaneously measured the quantity and quality of extracellular mitochondria. Next, by priming mouse macrophages with isolated healthy and damaged mitochondria, we determined if damaged extracellular mitochondria are capable of inducing tolerance to subsequent endotoxin challenge. Finally, we determined if inhibition of Drp1/Fis1-mediated pathologic fission abrogates release of damaged extracellular mitochondria and improves macrophage response to subsequent endotoxin challenge.

\* **Corresponding author:** Bereketeab Haileselassie MD MHS, Department of Pediatrics Division of Critical Care Medicine, Stanford University School of Medicine, Stanford, CA; bhailes3@stanford.edu, Telephone number:650-497-7894. Authors' contributions: R.M, B.H. and D.M-R contributed to manuscript preparation. R.M, B. H and D.M-R generated the hypothesis. T.C, M.H. and D.M-R aided with experimental design. R.M, B.H, C.M.T, N.P.O, A.U.J, L.M.M conducted experiments and/or helped with data analysis. All the authors reviewed and edited the manuscript.

**Results:** When compared to naïve macrophages (NM), endotoxin tolerant macrophages (ETM) demonstrated Drp1/Fis1-dependent mitochondrial dysfunction and higher levels of damaged extracellular mitochondria (MTG+events/50µl: ETM=2.42×10<sup>6</sup>±4391 vs NM=5.69 ×10<sup>5</sup>±2478; p<0.001). Exposure of naïve macrophages to damaged extracellular mitochondria (M<sub>H</sub>) induced cross tolerance to subsequent endotoxin challenge while healthy mitochondria (M<sub>C</sub>) had minimal effect (TNFα (pg/ml): NM=668±3, NM+M<sub>H</sub>=221±15 and NM+M<sub>C</sub>=881±15; p<0.0001). Inhibiting Drp1/Fis1-dependent mitochondrial fission using P110, a selective inhibitor of Drp1/Fis1 interaction, improved extracellular mitochondrial function (extracellular mitochondrial membrane potential, JC-1(R/G) ETM=7±0.5 vs ETM+P110=19.±2.0; p<0.001) and subsequently improved immune response in endotoxin tolerant macrophages (TNFα (pg/ml); ETM=149±1 vs ETM+P110=1150±4; p<0.0001). Similarly, P110-treated endotoxin tolerant mice had lower amounts of damaged extracellular mitochondria in plasma (represented by higher extracellular mitochondrial membrane potential, TMRM/MT-G: ET=0.04±0.02 vs ET+P110=0.21±0.02, p=0.03) and improved immune response to subsequent endotoxin treatment as well as cecal ligation and puncture.

**Conclusions:** Inhibition of Drp1/Fis1-dependent mitochondrial fragmentation improved macrophage function and immune response both *in vitro* and *in vivo* models of endotoxin tolerance. This benefit is mediated, at least in part, by decreasing the release of damaged extracellular mitochondria, which contributes to endotoxin cross tolerance. Altogether, these data suggest that alterations in mitochondrial dynamics may play an important role in sepsis-induced immunoparalysis.

### Keywords

Sepsis; Immunoparalysis; Extracellular mitochondria; Mitochondrial fission; DRP1

## INTRODUCTION

Advances in immune phenotyping have demonstrated significant variability in patients' immune response to acute infection, ranging from a hyper-inflammatory state associated with hemodynamic instability to profound immune-suppression and indolent end organ dysfunction (1,2,3). Currently, management of sepsis is focused on early source control along with supportive care for the clinical sequelae of the hyper-inflammatory state, which manifests as early hemodynamic instability (4). However, a more inclusive concept of 'immune dysregulation', which better reflects the dynamic nature of the host response to acute infection (5), has taken forefront in sepsis literature and highlights the impact of sepsis-induced immunoparalysis on late-stage morbidity and mortality (6).

Recent focus on cellular bioenergetics, has highlighted the impact of impaired mitochondrial dynamics on sepsis induced mitochondrial dysfunction (7,8,9,10). In particular, pathologic mitochondrial fragmentation, which is mediated through dynamin related protein 1 (DRP-1) hyperactivation and interaction with mitochondrial adaptor fission 1 (Fis1), has been linked to end organ failure in sepsis (11,12). Recently, Drp1/Fis1-dependent mitochondrial fragmentation has been shown to lead to the extracellular release of dysfunctional mitochondria in animal models of neurodegeneration (13). However, the link between

altered mitochondrial dynamics and extracellular mitochondrial content has not been explored in the context of sepsis induced immune-dysregulation.

Accordingly, using an *in vitro* and murine endotoxin tolerance models, as well as clinical samples from septic patients, we characterized changes in mitochondrial dynamics and subsequent extracellular mitochondrial content in sepsis-induced immunoparalysis. Furthermore, using a previously validated heptapeptide (P110) that selectively inhibits the binding of activated Drp1 to Fis1 (14), we determined whether blocking Drp1/Fis1-mediated excessive mitochondrial fission decreases release of dysfunctional mitochondria and improves macrophage function in endotoxin tolerance.

## METHODS

### *In Vitro* endotoxin tolerance model

Peritoneal derived murine macrophage cell line, RAW-264.7 cells (ATCC®-TIB-71™), were cultured in Dulbecco's Minimal essential Media (DMEM) (Corning-Cat#10013CV) supplemented with 10% fetal bovine serum (Gemini Bio-products). Cells were used at passage numbers between 6 and 14 for experiments. Bone marrow derived macrophages (BMDM) were attained from 6-week-old C57BL/6 mice using published protocol (15). These cells were incubated in media ± 10 ng/ml LPS (Sigma, Cat#L4391) for 16 hours to induce tolerance(16). The cells were then washed and treated with 1000 ng/ml LPS for 1–24 hours depending on the experimental requirement (16). Peptide P110 was used at 1µM concentration per previous protocols (11,12). Detailed methods for each in vitro assay are listed in the Supplementary Methods section.

### Murine Endotoxin tolerance model

*In vivo* endotoxin tolerance was performed using both LPS and Cecal ligation and puncture models(17,18). All animals received humane care in accordance with the Veterinary Service Center at Stanford University (AICUC protocol # 303321).

**LPS model:** BALB/c mice, 5–7 weeks of age, were acclimated for 1-week prior to procedures. Mice were initially treated with 1 mg/kg of LPS intraperitoneally for 18 hours to induce tolerance (17). Endotoxin-naïve (EN) and endotoxin-tolerized (ET) mice were subsequently treated with 10 mg/kg of LPS intraperitoneally (Fig. 5A). Drp1/Fis1 interaction was pharmacologically inhibited using peptide P110 at 0.5 mg/kg/day intraperitoneally per previous protocols (11,12). Control mice were treated with the same volume of pyrogen-free saline at the same time points. Plasma samples were collected 90 minutes after high dose endotoxin treatment to measure pro inflammatory cytokines TNF-α and IL-6 using commercially available ELISA (enzyme-linked immunosorbent assay) kits. Extracellular mitochondria were quantified in each treatment group 24 hours after high dose endotoxin treatment using flow cytometry. Methods for isolation and quantification of extracellular mitochondria as well as ELISA are detailed in supplementary methods section.

Cecal ligation and puncture (CLP) model: C57BL/6 mice, 5–7 weeks of age, were acclimated for 1-week prior to procedures. Endotoxin tolerance was induced by pre-treating mice with 5 mg/kg of LPS intraperitoneally 18 hours prior to CLP surgery (Fig. 5B) (18).

Peptide P110 was administered at 0.5mg/kg intraperitoneally to a subset of the animals per previous protocols (11,12). CLP surgery was performed by making a 1-cm midline laparotomy incision to expose the cecum and adjoin intestine. The cecum was then ligated tightly 5 mm from its base and subsequently punctured once with a sterile 18-gauge needle on the anti-mesenteric border. The bowel was then returned to the peritoneal cavity, and the abdominal incision was closed with a 4.0 silk suture. Similar to the LPS model, TNF- $\alpha$  and IL-6 levels were quantified using ELISA and extracellular mitochondria quantity and quality were measured using flow cytometry. Detailed methods found in supplementary.

### Patient samples

Blood samples were attained from a cohort of septic and healthy children enrolled in a immunophenotyping study at Nationwide Children's Hospital (19). The samples from septic children and healthy controls were collected under protocols approved by the Nationwide Children's Hospital Institutional Review Board (protocol ID: IRB10-00028, IRB11-00565). Innate immune function was assessed in all subjects through measurement of their whole blood *ex vivo* LPS-induced tumor necrosis factor (TNF)- $\alpha$  production capacity (TNF $\alpha$  response). A TNF $\alpha$  response >1,000 pg/ml is typical of healthy controls, while a TNF $\alpha$  response <200 pg/ml has been used to characterize critical illness-induced immune suppression (immunoparalysis) (19,20). Plasma from these patients was used to quantify extracellular mitochondrial DNA and protein. Quantification is described in detail in the Supplementary Methods.

## RESULTS

### Inhibition of Drp1/Fis1-mediated mitochondrial fragmentation limits mitochondrial dysfunction and improves endotoxin-tolerance.

Using a previously-validated rationally designed peptide (P110), which selectively inhibits Drp1/Fis1 interaction (11,12,13,14), we evaluated the impact of pathologic mitochondrial fragmentation on cellular respiration and immune function in the setting of endotoxin tolerance (16). Results from our *in vitro* model (Fig. S1A) demonstrated that P110-treated endotoxin tolerant macrophages (ETM +P110) had decreased Drp1 activation, represented by lower mitochondrial localization of Drp1, (Drp1 normalized to VDAC1: Control = 0.17 $\pm$ 0.02 vs ETM = 0.49 $\pm$ 0.05 vs ETM+P110 = 0.29 $\pm$ 0.01; p = 0.025) (Fig. 1A, S2A–D). P110-treated endotoxin tolerant macrophages also had approximately 60% decrease in mitochondrial ROS (MitoSox; ETM=0.029 $\pm$ 0.002 vs ETM+P110=0.010 $\pm$ 0.001; p<0.0001) and associated decrease in oxidative post translational modifications (s-nitrosylation; ETM=0.69 $\pm$ 0.09 vs ETM+P110=0.34 $\pm$ 0.04; p=0.03) (Fig. 1B, S3A–B). P110-treated endotoxin tolerant macrophages had also improved mitochondrial membrane potential (JC1 (R/G) (ETM+P110=38.8 $\pm$ 1.5 vs ETM=12.0 $\pm$ 0.4; p<0.0001) (Fig. 1C) as well as improved cellular respiration on seahorse oximetry (Basal respiration (pmol/min/ $\mu$ g): ETM+P110=6.8 $\pm$ 6.2 vs ETM=3.3 $\pm$ 0.8, p=0.03; Maximum respiration (pmol/min/ $\mu$ g): ETM+P110=14.1 $\pm$ 2.3 vs ETM=6.1 $\pm$ 1.3, p=0.03; and ATP-dependent respiration (pmol/min/ $\mu$ g): ETM+P110=4.4 $\pm$ 0.6 vs ETM=1.5 $\pm$ 0.3, p=0.01) (Fig. 1D, S3C).

Next, we evaluated the impact of inhibiting Drp1/Fis1 interaction on immune function. P110-treated endotoxin tolerant macrophages had appropriate immune response to acute endotoxin stimulation, represented by increased TNF $\alpha$  and IL-6 production (TNF $\alpha$  (pg/ml): ETM+P110=1150 $\pm$ 4 vs ETM=149 $\pm$ 1;  $p$ <0.0001; IL-6 (pg/ml): ETM+P110=128 $\pm$ 7 vs ETM=0.0;  $p$ <0.001), increased phagocytosis (bioparticle uptake (%): ETM+P110=68 $\pm$ 2 vs ETM=9 $\pm$ 4;  $p$ <0.0001) and increased nitric oxide production (NO $_2^-$  ( $\mu$ M): ETM+P110=0.093 $\pm$ 0.004 vs ETM=0.053 $\pm$ 0.004;  $p$ <0.0001) (Fig. 2A–D). Evaluation of canonical signaling pathways, which mediate endotoxin tolerance (21,22) demonstrated that P110-treated endotoxin tolerant macrophages had an appropriate increase in NF $\kappa$ B activation and nuclear localization following LPS stimulation (NF $\kappa$ B/Histone-H3: ETM+P110=0.381 $\pm$ 0.08 vs ETM=0.1233 $\pm$ 0.001;  $p$ =0.01). Furthermore, P110-treated endotoxin tolerant macrophages had a significant decrease in IRAK-M (IRAK-M/ $\beta$ -actin: ETM+P110=0.9 $\pm$ 0.1 vs ETM=1.9 $\pm$ 0.1;  $p$ <0.0001), which is a key serine/threonine kinase known to regulate endotoxin tolerance (22) (Fig. 2E).

These results were validated *in vivo* using two different murine models of endotoxin tolerance (ET) (17,18). P110-treated endotoxin tolerized mice (ET+P110) had an appropriate pro-inflammatory response to acute LPS stimulation (TNF $\alpha$  (pg/ml): ET+P110=1453 $\pm$ 91 vs ET=134 $\pm$ 16;  $p$ <0.0001; IL-6 (pg/ml): ET+P110=2216 $\pm$ 107.3 vs ET=342 $\pm$ 41;  $p$ <0.0001) (Fig 3A–C) as well as to cecal ligation and puncture (TNF $\alpha$  (pg/ml): ET+P110=510 $\pm$ 18 vs ET=46 $\pm$ 10;  $p$ <0.0001; IL-6 (pg/ml): ET+P110=2842 $\pm$ 19 vs ET=86 $\pm$ 40;  $p$ <0.0001) (Fig 3D–F).

### Pharmacological inhibition of Drp1/Fis1-mediated mitochondrial fragmentation attenuates the release of damaged mitochondria to the extracellular milieu in endotoxin tolerance model.

Recently, our group as well as others have demonstrated that excessive mitochondrial fission mediates release of damaged mitochondria in response to cytotoxic cues (13,23) and that mitochondrial byproducts can mediate endotoxin cross tolerance by activating different pattern recognition receptors (24). Accordingly, we sought to determine whether the protective effect of P110 is mediated by decreasing the release of damaged extracellular mitochondria to induce endotoxin cross tolerance. We first quantified the amounts of extracellular mitochondria in our *in vitro* and *in vivo* models of endotoxin tolerance. When compared to naïve macrophages (NM), endotoxin tolerant macrophages (ETM) had higher amounts of extracellular mitochondria, quantified by using flow cytometry (MTG+events/50 $\mu$ l: ETM=2.42 $\times$ 10 $^6$  $\pm$ 4,000 vs ENM=5.7 $\times$ 10 $^5$  $\pm$ 2,500;  $p$ <0.001), as well as mitochondrial byproducts, including mitochondrial proteins (VDAC1/ $\mu$ l (A.U.): ETM=360 $\pm$ 20 vs NM=209 $\pm$ 13,  $p$ <0.01; Tim23/ $\mu$ l (A.U.): ETM=207 $\pm$ 13 vs NM=47 $\pm$ 4;  $p$ <0.001) and mitochondrial DNA (mtDNA/nucDNA: ETM=60 $\pm$ 6 vs NM=32 $\pm$ 5;  $p$ =0.02) (Fig. S4B–F). These findings were further validated in murine models, demonstrating that endotoxin tolerant (ET) mice have more cell free mitochondria in plasma when compared to endotoxin naïve (EN) mice (LPS model: MTG+events/50 $\mu$ l: ET=2.9 $\times$ 10 $^4$  $\pm$ 9,700 vs EN=5.600 $\pm$ 3,  $p$ =0.02; CLP model: MTG+events/50 $\mu$ l: ET=1.04 $\times$ 10 $^5$  $\pm$ 34,000 vs EN=3.03 $\times$ 10 $^4$  $\pm$ 8188,  $p$ =0.04) (Fig. S5B,D).

To determine the clinical relevance of these findings, we quantified extracellular mitochondrial content in a pilot cohort of septic children who were stratified by immune function, using whole blood *ex-vivo* TNF $\alpha$  response (19). Per previous literature, TNF $\alpha$  response below 200 pg/ml was used to classify patients as immunoparalyzed (IP) (19,25) (Fig S6A). Our results demonstrated an increase in extracellular mitochondrial protein (VDAC1/ $\mu$ l (A.U.): IP= $2.1 \times 10^5 \pm 5,800$  vs IC= $8.0 \times 10^4 \pm 1,000$  p=0.03) (Fig S6B–D) as well as extracellular mitochondrial DNA (mtDNA/nucDNA: IP= $6.6 \pm 1.4$  vs IC= $2.4 \pm 0.4$ ; p=0.01) (Fig S6B–E) in the plasma of immunoparalyzed (IP) septic patients, when compared to immunocompetent (IC) septic patients.

When evaluating extracellular mitochondrial morphology using electron microscopy, our results demonstrated significant distortion of mitochondrial architecture, suggestive of mitochondrial damage in endotoxin-tolerant macrophages following high dose LPS stimulation (Fig. 4A, S7A–B). This is further supported by the lower membrane potential of extracellular mitochondria from endotoxin-tolerant macrophages (ETM) when compared to naïve macrophages (NM) (JC-1(R/G): ETM= $6.9 \pm 0.5$  vs NM= $14.3 \pm 0.3$ ; p=0.03) (Fig. 4B). Similarly, extracellular mitochondria found in the plasma of endotoxin tolerant (ET) mice demonstrated a significant decrease in membrane potential when compared to endotoxin naïve (EN) mice in both LPS and CLP models (LPS model: TMRM/MT-G: ET= $0.13 \pm 0.02$  vs EN= $0.22 \pm 0.02$ , p=0.03; CLP model: TMRM/MT-G: ET= $0.04 \pm 0.02$  vs EN= $0.30 \pm 0.05$ ; p<0.01) (Fig. 4C–D, S5A,C).

Finally, we evaluated the impact of P110 treatment on the quantity and function of extracellular mitochondria in our models of endotoxin tolerance. Results from these experiments demonstrated that extracellular mitochondria from P110-treated endotoxin tolerant macrophages had a higher mitochondrial membrane potential in vitro (JC-1(R/G): ETM+P110= $19 \pm 2$  vs ETM= $6.9 \pm 0.5$ ; p<0.001). This was further validated in the murine models, which demonstrated improved extracellular mitochondrial membrane potential in P110-treated endotoxin tolerant mice (LPS model: TMRM/MT-G: ET+P110= $0.24 \pm 0.02$  vs ET= $0.15 \pm 0.02$ , p=0.02; CLP model: TMRM/MT-G: ET+P110= $0.21 \pm 0.02$  vs ET= $0.04 \pm 0.02$ ; p=0.03) (Fig. 4B–D). However, as we found before in a model of neuroinflammation (13), P110 treatment did not significantly impact the amounts of extracellular mitochondria (LPS model: MTG+ events/50  $\mu$ l: ET+P110= $2.3 \times 10^4 \pm 8,000$  vs ET= $2.9 \times 10^4 \pm 9,700$ , p=0.6; CLP model: MTG+ events/50  $\mu$ l: ET+P110= $6.3 \times 10^4 \pm 13,000$  vs ET= $1.04 \times 10^5 \pm 34,000$ ; p=0.3) (Fig S5B,D).

### **Damaged extracellular mitochondria induce tolerance to subsequent endotoxin exposure.**

Since our results suggest that inhibition of Drp1/Fis1-mediated pathologic fission influences the quality of extracellular mitochondria, we sought to determine if damaged extracellular mitochondria can induce endotoxin tolerance. We first pre-treated naïve macrophages with cell supernatant from healthy cells as well as cells that had mitochondrial damage (Fig 5A). Mitochondrial damage was induced using two independent mechanisms: LPS treatment, S(L) and hydrogen peroxide treatment, S(H) (Fig S8A–B) (26), to address potential confounding due to LPS transfer in the supernatant.

Our results demonstrated that naïve macrophages treated with supernatant from damaged cells, (S(L) or S(H)), developed tolerance to subsequent endotoxin challenge, represented by decreased TNF $\alpha$  and IL-6 production compared to macrophages pre-treated with supernatant from healthy cells (S(C)) (TNF $\alpha$  (pg/ml): S(L)=98 $\pm$ 3 vs S(H)=113 $\pm$ 2 vs S(C)=668 $\pm$ 3,  $p$ <0.0001; IL-6 (pg/ml): S(L)=29 $\pm$ 7 vs S(H)=66 $\pm$ 5 vs S(C)=496 $\pm$ 48,  $p$ <0.0001) (Fig. 5B–C). To address the possibility that other cellular biproducts found in transferred supernatant can induce tolerance, we treated naïve macrophages with isolated healthy (M<sub>C</sub>) and damaged (M<sub>H</sub>) mitochondria and subsequently challenged these cells with endotoxin (Fig S8C). Results from this experiment demonstrated that treatment with damaged mitochondrial (M<sub>H</sub>) prior to endotoxin challenge, induced tolerance phenotype while treatment with healthy mitochondria (M<sub>C</sub>) had minimal detrimental impact (TNF $\alpha$  (pg/ml): M<sub>H</sub>=221 $\pm$ 15 vs M<sub>C</sub>=881 $\pm$ 15;  $p$ <0.0001) (Fig. S8D).

Multiple mitochondrial biproducts have been implicated in mediating cross tolerance to endotoxin (27,28). In particular, methylated CpG of mitochondrial DNA (mtDNA) has been shown to mediate cross tolerance (24). To determine if pathologic fission-mediated release of mtDNA is a key driver of tolerance in our model, we removed extracellular mtDNA by deoxyribonuclease (DNase) treatment in our supernatant transfer experiment (represented by nomenclature S(H)- DNA in Fig 5A). Similarly, to understand the effect of intact extracellular mitochondria, we removed mitochondria from the supernatant prior to transfer (represented by nomenclature S(H)- mito in Fig 5A), using high speed centrifugation and filtration. Results from this experiment demonstrated that DNase treatment of supernatant (S(H)- DNA) partially reversed tolerance to subsequent LPS challenge, whereas removal of mitochondria by centrifugation and filtration (S(H)- mito) led to a near complete reversal of tolerance (TNF $\alpha$  (pg/ml); S(H)=115 $\pm$ 3 vs S(H)- DNA=318 $\pm$ 7 vs S(H)- mito=626 $\pm$ 5;  $p$ <0.01; IL-6 (pg/ml); S(H) =115 $\pm$ 3 vs S(H)- DNA=318 $\pm$ 7 vs S(H)- mito=625 $\pm$ 5;  $p$ =0.04) (Fig. 5B–C).

## DISCUSSION

Although mitochondrial dysfunction has been previously associated with immunoparalysis in the sepsis literature (29,30), the role of altered mitochondrial dynamics and its impact on extracellular mitochondrial content has not been fully explored in this context. As a result of their bacterial ancestry, mitochondria contain structural elements that are recognized by pathogen recognition receptors (PRR) of the innate immune system (31). These PRRs, which respond to mitochondrial biproducts, have also been shown to mediate cross tolerance to endotoxin (32). Thus, the presence of extracellular mitochondria and associated biproducts in the circulation of septic patients likely contributes to the immune dysregulation, which is often observed. Our results demonstrate that Drp1/Fis1-dependent pathologic mitochondrial fragmentation is a key upstream mechanism in the release of damaged mitochondria and associated biproducts. Furthermore, we demonstrate that loss of structural and functional integrity of extracellular mitochondria plays a significant role in its immunogenicity. Finally, selective inhibition of Drp1/Fis1 interaction with P110 reverses the impairments in macrophage bioenergetics, decreases the release of dysfunctional mitochondria and limits the endotoxin tolerance phenotype, both *in vitro* as well as in animal models of sepsis.

## **Drp1/Fis1-dependent mitochondrial dysfunction mediates endotoxin tolerance through damaged extracellular mitochondria**

While the link between metabolism and immune response is widely appreciated, less is known regarding the impact of mitochondrial dynamics on immune phenotypes. Recent publications have shown that mitochondria confer specific morphologies in accordance to the immune cell activation state (13,33,34). Furthermore, modifying key regulators of mitochondrial fission and fusion machinery influences immune cell metabolism by augmenting mitochondrial health (24,34). Our current findings, which demonstrate that inhibition of Drp1/Fis1-mediated pathologic fission improves cellular respiration and immune function in endotoxin-tolerant macrophages, further supports the importance of mitochondrial dynamics in innate immune metabolism. Additionally, our findings show that Drp1/Fis1-mediated pathologic fission can promote the release of damaged mitochondria and associated byproducts, thus identifying an alternate mechanism by which alterations in mitochondrial dynamics could modulate innate immune phenotypes.

At this time, the mechanisms which mediate mitochondrial release to the extracellular space are still under investigation. Passive release of cellular byproducts has been well described in the setting of cell death (necrosis, necroptosis, pyroptosis) (35,36,37). However, our data demonstrate that the release of mitochondria from macrophages is occurring in a cell death-independent manner (SIH), suggesting an active process. Recent evidence has demonstrated that mitochondrial release can occur *via* direct exocytosis or via extracellular vesicles (EVs), (38,39), both of which are feasible mechanisms in innate immune cells and thus require further investigation.

## **The structural and functional integrity of extracellular mitochondria influences immune response**

In addition to increased abundance, we found that released mitochondria from endotoxin tolerant macrophages have significant impairments in structural and functional integrity, confirmed by measuring mitochondrial membrane potential and with electron microscopy (Fig. 4, S7). While these damaged extracellular mitochondria were found to have detrimental impact on macrophage function, healthy extracellular mitochondria had minimal detrimental effect (Fig. S8C–D). Furthermore, Drp1/Fis1 inhibition improved the structural and functional integrity of extracellular mitochondria (Fig 4B–D), with minimal effect on the amounts of extracellular mitochondria (Fig. S5B,D). Altogether, these findings suggest that structural and functional integrity of extracellular mitochondria play a role in eliciting an immune response. We believe this to be a notable finding since the impact of extracellular mitochondria has been debated in recent literature, with publications demonstrating both a protective (10,40) and detrimental role (41,42) in various animal models. Based on our results, we speculate that the integrity and functional status of the extracellular mitochondria is one of the key variables, which determine their impact.

## **Limitations and future directions:**

Although our study suggests that Drp1/Fis1-dependent mitochondrial fragmentation is an important mediator of macrophage dysfunction in endotoxin tolerance, there are limitations to our study. One fundamental limitation arises from the immortalized, as well as primary



murine, cell lines utilized within these experiments. RAW-264.7 cells, as well as bone marrow-derived macrophages were selected for this study as they have been extensively used in sepsis models and to avoid inter subject variability that can influence inflammatory response in ex vivo models of human monocytes (43,44). However, we recognize that future clinical studies are necessary to validate our findings in septic patients. We also recognize that, while there is significant pre-clinical efficacy and safety data for peptide P110 (45), future studies are necessary to validate this therapeutic target.

## Conclusion

Our findings suggest that inhibition of Drp1/Fis1-dependent pathological mitochondrial fission improves macrophage function *in vitro* and in our murine models of endotoxin tolerance. This correlates with a decrease in the release of damaged mitochondria to the extracellular milieu, and with endotoxin cross-tolerance. Thus, treatments that abrogate pathological fission and improve the quality of extracellular mitochondria may have therapeutic potential in sepsis as well as other inflammatory disorders.

## Supplementary Material

Refer to Web version on PubMed Central for supplementary material.

## Acknowledgements:

This work was supported by NICHD K99 HD099387, and Maternal Child Research Institute MCHRI pilot grant to BH and HL52141 to DM-R. The authors thank John Perrino for technical support with EM and Lisa Nichols and Meredith Weglarz for technical support with flow cytometry.

## Copyright Form Disclosure:

Drs. Massis, Vijayan, Monack, Mochly-Rosen, and Haileselassie received support for article research from the National Institutes of Health (NIH). Dr. Hall received funding from La Jolla Pharmaceuticals. Dr. Mochly-Rosen's institution received funding from the NIH (HL52141 RO1 grant). Dr. Haileselassie received support for article research from the Stanford Maternal Child Research Institute pilot grant. The remaining authors have disclosed that they do not have any potential conflicts of interest.

## References:

1. Kellum JA, Kong L, Fink MP, et al. : Understanding the inflammatory cytokine response in pneumonia and sepsis: results of the Genetic and Inflammatory Markers of Sepsis (GenIMS) Study. *Archives of Internal Medicine* 2007; 167: 1655–1663. [PubMed: 17698689]
2. Hartman ME, Linde-Zwirble WT, Angus DC, et al. : Trends in the epidemiology of pediatric severe sepsis. *Ped Crit Care Med* 2013; 14: 686–93.
3. Typpo K, Watson RS, Bennett TD, et al. : Outcomes of Day 1 Multiple Organ Dysfunction Syndrome in the PICU. *Ped Crit Care Med* 2019; 20: 914–22.
4. Weiss SL, Peters MJ, Alhazzani W, et al. : Surviving Sepsis Campaign International Guidelines for the Management of Septic Shock and Sepsis-Associated Organ Dysfunction in Children. *Ped Crit Care Med* 2020; 21: e52–e106.
5. Delano MJ, Ward PA: Sepsis-induced immune dysfunction: can immune therapies reduce mortality? *J. Clin. Invest* 2016; 126: 23–31. [PubMed: 26727230]
6. Hall MW, Knatz NL, Vetterly C, et al. : Immunoparalysis and nosocomial infection in children with multiple organ dysfunction syndrome. *Int Care Med* 2011; 37: 525–532.
7. Weiss SL, Selak MA, Tuluc F, et al. : Mitochondrial dysfunction in peripheral blood mononuclear cells in pediatric septic shock. *Ped Crit Care Med* 2015; 16: e4–e12.

8. Weiss SL, Zhang D, Bush J, et al. : Persistent mitochondrial dysfunction linked to prolonged organ dysfunction in pediatric sepsis. *Crit Care Med* 2019; 47: 1433–1441. [PubMed: 31385882]
9. McBride MA, Owen AM, Stothers CL, et al. : The Metabolic Basis of Immune Dysfunction Following Sepsis and Trauma. *Front Immunol* 2020; 11: 1–21. [PubMed: 32038653]
10. Hayakawa K, Esposito E, Wang X, et al. : Transfer of mitochondria from astrocytes to neurons after stroke. *Nature* 2016; 535, 551–555. [PubMed: 27466127]
11. Haileselassie B, Mukherjee R, Joshi AU, et al. : Drp1/Fis1 interaction mediates mitochondrial dysfunction in septic cardiomyopathy. *J Mol Cell Cardiol* 2019; 130: 160–169. [PubMed: 30981733]
12. Haileselassie B, Joshi AU, Minhas PS, et al. : Mitochondrial dysfunction mediated through dynamin-related protein 1 (Drp1) propagates impairment in blood brain barrier in septic encephalopathy. *J Neuroinflam* 2020; 17: 1–11.
13. Joshi AU, Minhas PS, Liddelov SA, et al. : Fragmented mitochondria released from microglia trigger A1 astrocytic response and propagate inflammatory neurodegeneration. *Nat Neuro* 2019; 22: 1635–1648.
14. Qi X, Qvit N, Su YC, et al. : A novel Drp1 inhibitor diminishes aberrant mitochondrial fission and neurotoxicity. *J Cell Sci.* 2013; 126: 789–802. [PubMed: 23239023]
15. Trouplin V, Boucherit N, Gorvel L, et al. : Bone marrow-derived macrophage production. *J. Vis. Exp* 2013; 81: e50966.
16. Xiang Q, Wen L, Liu MH, et al. : Endotoxin tolerance of RAW264.7 correlates with p38-dependent up-regulation of scavenger receptor-A. *J Int Med Res.* 2009; 37:491–502. [PubMed: 19383244]
17. Lehner MD, Ittner J, Bundschuh DS, et al. : Improved innate immunity of endotoxin-tolerant mice increases resistance to *Salmonella enterica* serovar typhimurium infection despite attenuated cytokine response. *Infection and immunity* 2001; 69: 463–471. [PubMed: 11119538]
18. Wheeler DS, Lahni PM, Denenberg et AG. al: Induction of endotoxin tolerance enhances bacterial clearance and survival in murine polymicrobial sepsis. *Shock* 2008; 30: 267–273. [PubMed: 18197145]
19. Muszynski JA, Nofziger R, Moore-Clingenpeel M, et al. : Early immune function and duration of organ dysfunction in critically III children with sepsis. *Am. J. Resp. Crit. Care Med* 2018; 198: 361–369. [PubMed: 29470918]
20. Weiss SL, Zhang D, Bush J, et al. : Mitochondrial dysfunction is associated with an immune paralysis phenotype in pediatric sepsis. *Shock* 2020; 54: 285–293. [PubMed: 31764621]
21. Hobbs S, Reynoso M, Geddis AV, et al. : LPS-stimulated NF- $\kappa$ B p65 dynamic response marks the initiation of TNF expression and transition to IL-10 expression in RAW 264.7 macrophages. *Physiol Rep.* 2018; 6:e13914. [PubMed: 30426723]
22. Liu ZJ, Yan LN, Li XH, et al. : Up-regulation of IRAK-M is essential for endotoxin tolerance induced by a low dose of lipopolysaccharide in Kupffer cells. *J Surg Res.* 2008; 150:34–9. [PubMed: 18533191]
23. Pollara J, Edwards RW, Lin L, et al. : Circulating mitochondria in deceased organ donors are associated with immune activation and early allograft dysfunction. *JCI Insight*, 2018;3: e121622.
24. Bao D, Zhao J, Zhou X, et al. : Mitochondrial fission-induced mtDNA stress promotes tumor-associated macrophage infiltration and HCC progression. *Oncogene.* 2019; 38:5007–5020. [PubMed: 30894684]
25. Weiss SL, Zhang D, Bush J, et al. : Mitochondrial dysfunction is associated with an immune paralysis phenotype in pediatric sepsis. *Shock* 2020; 54:285–293. [PubMed: 31764621]
26. Qin T, Ren Z, Liu X, et al. : Study of the selenizing Codonopsis pilosula polysaccharides protects RAW264.7 cells from hydrogen peroxide-induced injury. *Int J Biol Macromol.* 2019; 125:534–543. [PubMed: 30521910]
27. Harrington JS, Choi AMK, Nakahira K: Mitochondrial DNA in sepsis. *Curr.Op.Crit. Care*,2017; 23, 284–290.
28. Wenceslau CF, McCarthy CG, Szasz T, et al. : Mitochondrial N-formyl peptides induce cardiovascular collapse and sepsis-like syndrome. *Am. J. Physiol. Heart Circ. Physiol* 2015; 308:H768–H777. [PubMed: 25637548]

29. Protti A, Singer M. Bench-to-bedside review: potential strategies to protect or reverse mitochondrial dysfunction in sepsis-induced organ failure. *Crit Care*. 2006; 10:228. [PubMed: 16953900]
30. Park DW, Zmijewski JW. Mitochondrial Dysfunction and Immune Cell Metabolism in Sepsis. *Infect Chemother*. 2017; 49:10–21. [PubMed: 28378540]
31. Nakahira K, Hisata S, Choi AM. The roles of mitochondrial damage-associated molecular patterns in diseases. *Antioxid. Redox Signal* 2015; 23, 1329–1350. [PubMed: 26067258]
32. Julian MW, Strange HR, Ballinger MN, et al. : Tolerance and Cross-Tolerance following Toll-Like Receptor (TLR)-4 and –9 Activation Are Mediated by IRAK-M and Modulated by IL-7 in Murine Splenocytes. *PLoS One*. 2015; 10:e0132921. [PubMed: 26218271]
33. Garaude J, Acin-Perez R, Martinez-Cano S, et al. : Mitochondrial respiratory-chain adaptations in macrophages contribute to antibacterial host defense. *Nat. Immunol* 2016; 17:1037–1045. [PubMed: 27348412]
34. Mills EL, Kelly B, O’Neill LA: Mitochondria are the powerhouses of immunity. *Nat. Immunol* 2017; 18:488–498. [PubMed: 28418387]
35. Jahr S, Hentze H, Englisch S, et al. : DNA fragments in the blood plasma of cancer patients: quantitations and evidence for their origin from apoptotic and necrotic cells. *Cancer Res*. 2001; 61:1659–65. [PubMed: 11245480]
36. Jackson NL, Coke R, Kwong AC, et al. : Comparison of the source and prognostic utility of cfDNA in trauma and sepsis. *Intensive Care Med Exp*. 2019; 7:29. [PubMed: 31119471]
37. Denning NL, Aziz M, Gurien SD, et al. : DAMPs and NETs in Sepsis. *Front Immunol*. 2019; 10:2536. [PubMed: 31736963]
38. van Niel G, D’Angelo G, Raposo G: Shedding light on the cell biology of extracellular vesicles. *Nat. Rev. Mol. Cell. Biol* 2018; 19:213–228. [PubMed: 29339798]
39. Hessvik NP, Llorente A: Current knowledge on exosome biogenesis and release. *Cell Mol Life Sci*. 2018; 75:193–208. [PubMed: 28733901]
40. Islam MN, Das SR, Emin MT, et al. : Mitochondrial transfer from bone-marrow–derived stromal cells to pulmonary alveoli protects against acute lung injury. *Nat. Med*. 2012; 18:759–765. [PubMed: 22504485]
41. Scozzi D, Ibrahim M, Liao F, et al. : Mitochondrial damage-associated molecular patterns released by lung transplants are associated with primary graft dysfunction. *Am J Transplant*. 2019; 19:1464–1477. [PubMed: 30582269]
42. Lin L, Xu H, Bishawi M, et al. : Circulating mitochondria in organ donors promote allograft rejection. *Am. J. Transplant* 2019; 19:1917–1929. [PubMed: 30761731]
43. Mälarstig A, Siegbahn A: The intersubject variability of tissue factor mRNA production in human monocytes—relation with the toll-like receptor 4. *Thrombosis Res*. 2007; 120:407–413.
44. Danis VA, Millington M, Hyland VJ, et al. : Cytokine production by normal human monocytes: inter- subject variation and relationship to an IL- 1 receptor antagonist (IL- 1Ra) gene polymorphism. *Clin. Exp. Immunol* 1995; 99:303–310. [PubMed: 7851026]
45. Disatnik MH, Joshi AU, Saw NL, et al. : Potential biomarkers to follow the progression and treatment response of Huntington’s disease. *Journal of Experimental Medicine*. 2016; 213(12), 2655–2669. [PubMed: 27821553]

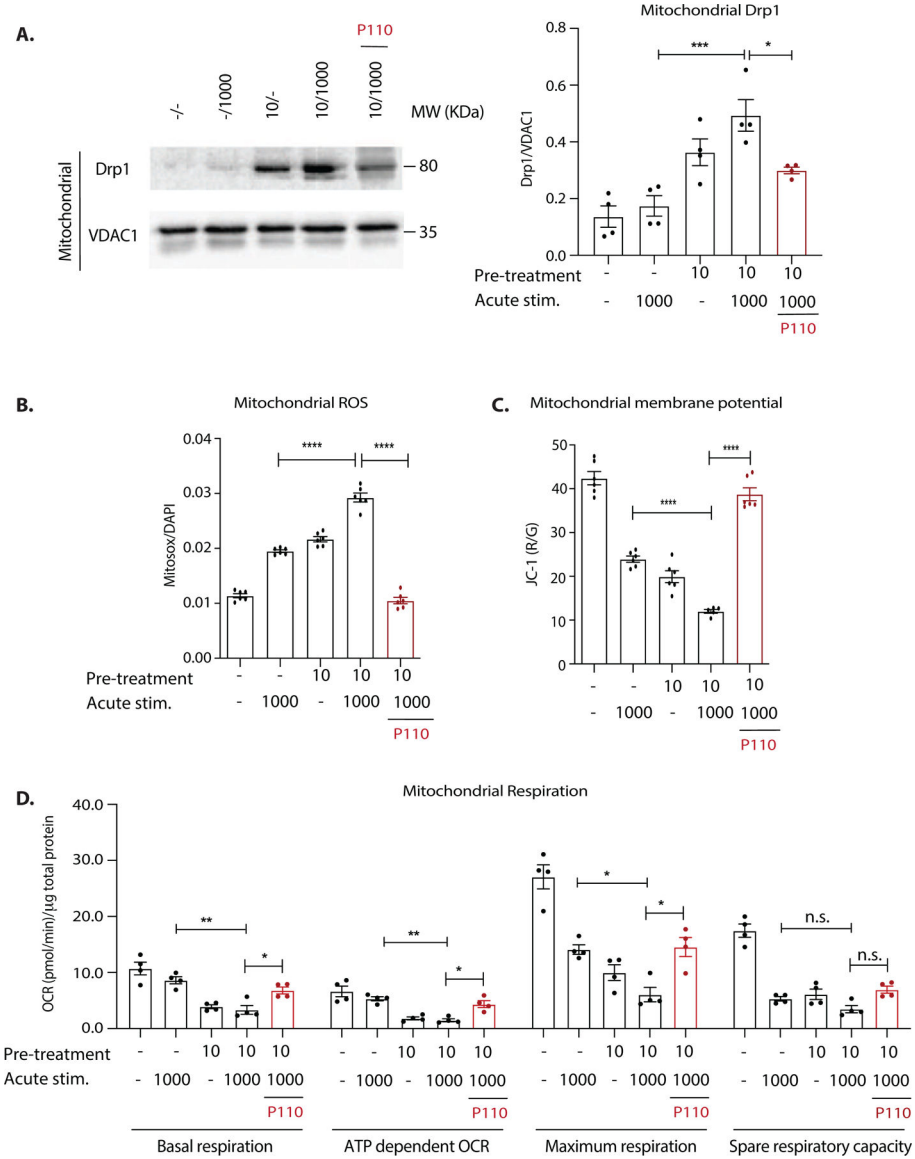


**Figure 1. Pharmacological inhibition of Drp1/Fis1 interaction abrogates mitochondrial damage in endotoxin tolerant macrophages.**

*In vitro* endotoxin tolerance model using RAW264.7 cells. Cells were pre-treated with low dose LPS (10ng/ml) for 16 hrs. to induce tolerance. Subsequently, macrophages were treated with high dose LPS (1000ng/ml). P110 treatment was given along with low dose LPS. (For experimental schematic see Supplemental figure S1A.) **(A)** Mitochondrial localization of Drp1 was measured by quantifying Drp1 in the mitochondrial enriched fraction (N=4). VDAC1, an outer mitochondrial membrane protein, was used as the loading control. Quantification of mitochondrial Drp1, presented as a ratio to VDAC1 in mitochondria-enriched lysate. **(B)** Mitochondrial ROS burden was measured by as a ratio of MitoSOX™ fluorescence to DAPI staining (N=6). **(C)** Mitochondrial membrane potential was measured by JC-1 fluorometric dye (N=6). **(D)** Cellular respiration was measured by changes in oxygen consumption rate, using Seahorse XF-24e to calculate basal respiration, ATP-dependent oxygen consumption, maximum respiration and spare respiratory capacity

(N=4), all presented in pmol/min/ $\mu$ g of protein. Analysis was performed using one-way ANOVA along with Tukey's multiple comparisons test. \* $p$  0.05; \*\* $p$  0.01; \*\*\* $p$  0.001; \*\*\*\* $p$  0.0001 and n.s. denoting not significant. N represents the number of independent experiments.

Author Manuscript

Author Manuscript

Author Manuscript

Author Manuscript

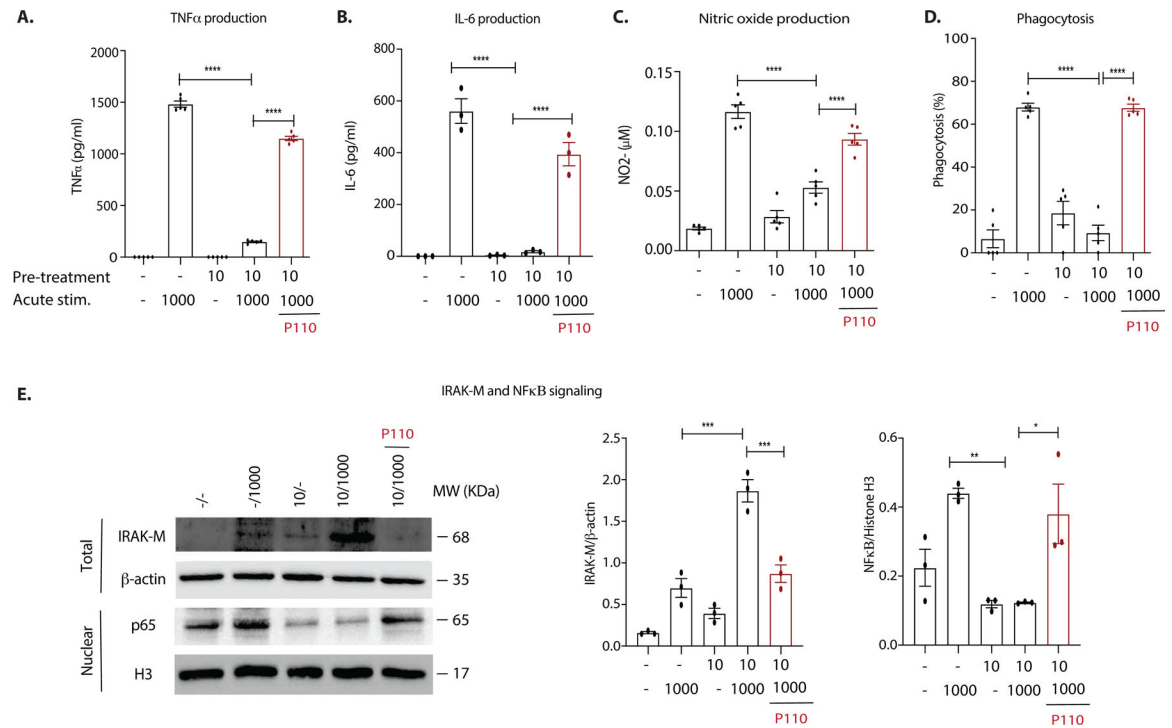


**Figure 2. Pharmacological inhibition of Drp1/Fis1 interaction improves immune function in endotoxin tolerant macrophages.**

Assessment of immune function in the endotoxin tolerant macrophages following P110 treatment was performed by measuring (A) TNF $\alpha$  production (N=6); (B) IL-6 production (N=3); (C) nitric oxide production (N=5); and, (D) phagocytotic capacity (N=5). (E) Evaluation of IRAK-M levels in total cell lysates as well as NF- $\kappa$ B nuclear localization by western blot. IRAK-M levels was quantified as a ratio of IRAK-M to  $\beta$ -actin in total cell lysate while NF- $\kappa$ B nuclear localization was quantified as a ratio of NF- $\kappa$ B to histone H3 in nuclear enriched lysate. Analysis was performed using one-way ANOVA along with Tukey's multiple comparisons test. \* $p$  0.05; \*\* $p$  0.01; \*\*\* $p$  0.001 and \*\*\*\* $p$  0.0001. N represents the number of independent experiments.

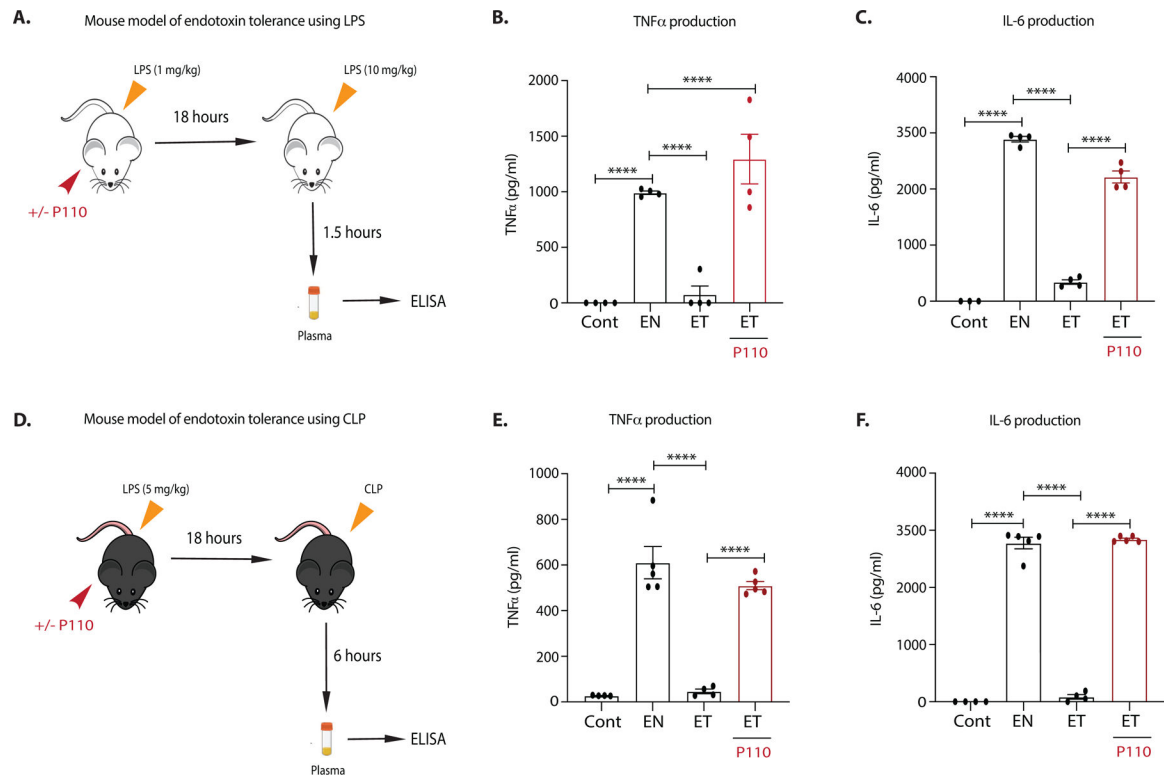


**Figure 3. Pharmacological inhibition of Drp1/Fis1 interaction improves immune response in endotoxin tolerance mouse model.**

(A) Schematic of endotoxin tolerance mouse model using LPS  $\pm$  P110. BALB/C mice were first treated with LPS (1mg/kg)  $\pm$  P110 for 18hrs. to induce tolerance. Mice subsequently received high dose LPS (10mg/kg) and pro inflammatory response was evaluated. (B). TNF $\alpha$  (N=4) and (C) IL-6 levels (N=4) levels quantified using ELISA. Results were validated using an alternate endotoxin tolerance mouse model. (D) As displayed on the schematic, C57BL/6J mice were treated with LPS (5mg/kg)  $\pm$  P110 for 18hrs to induce tolerance. Mice subsequently underwent cecal ligation and puncture. Pro-inflammatory cytokines (E) TNF $\alpha$  levels (N=5) and (F) IL-6 (N=5) were measured in mouse plasma 6 hours after CLP surgery. Analysis was performed using one-way ANOVA along with Tukey's multiple comparisons between each treatment group. \* $p$  0.05; \*\* $p$  0.01; \*\*\* $p$  0.001 and \*\*\*\* $p$  0.0001. N represents the number of independent experiments.

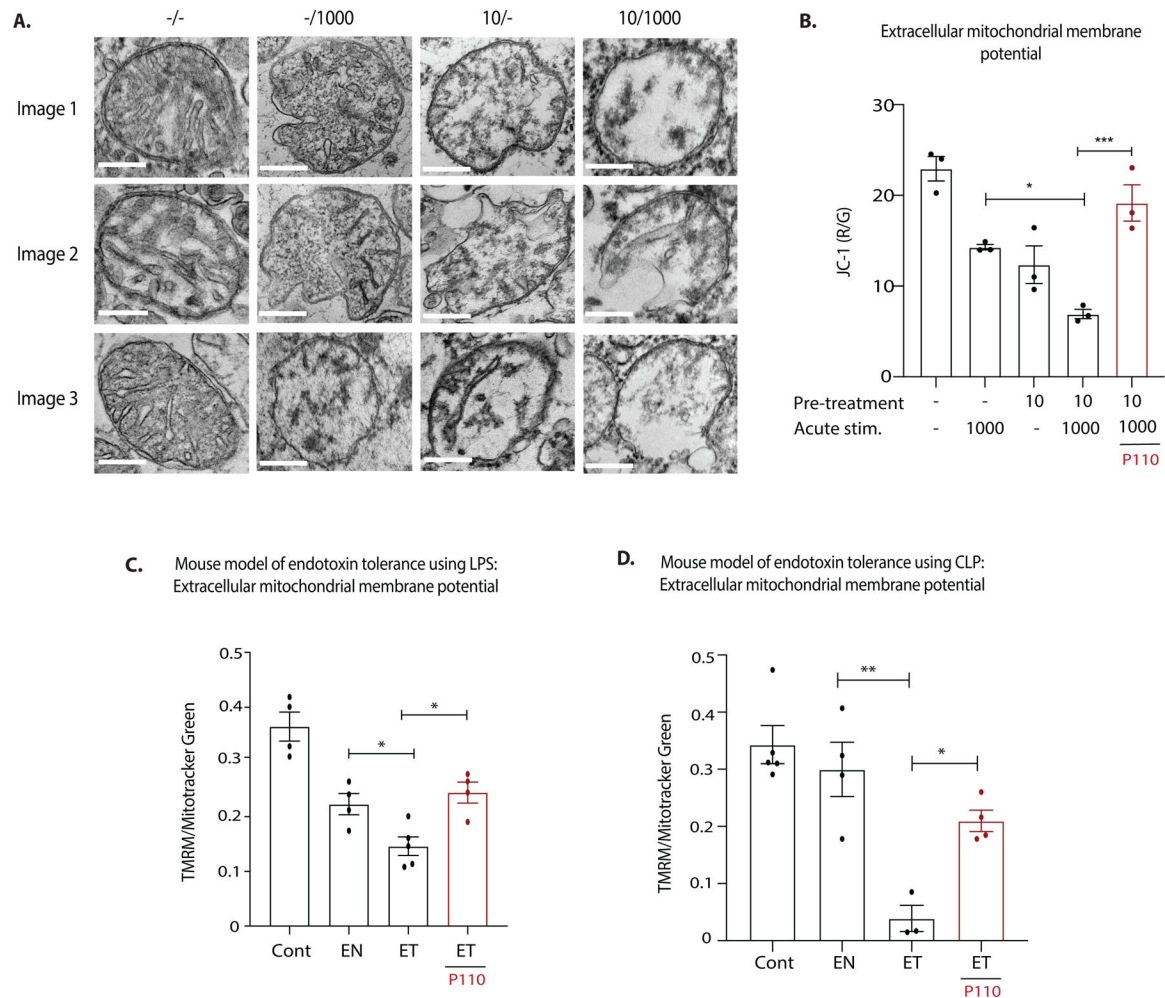


**Figure 4. Pharmacological inhibition of Drp1/Fis1 interaction limits release of damaged mitochondria to the extracellular milieu in cultured macrophages as well as mouse model of endotoxin tolerance.**

(A) Evaluation of extracellular mitochondria from our *in vitro* endotoxin tolerance model using electron microscopy. Three representative images are shown from each treatment group. Scale bar: 500 nm. (B) Membrane potential of extracellular mitochondria, collected from equal volumes of cell supernatants across all conditions and assessed using JC-1 fluorescent dye (N=3). Quantification of JC-1 was done as a ratio of Red (polarized) to green (depolarized) fluorescence. *In vivo* results were validated using both LPS (C) and CLP (D) model of endotoxin tolerance, in which extracellular mitochondrial membrane potential was evaluated using TMRM fluorescent dye by flow cytometry. Extracellular mitochondrial membrane potential normalized to total number of mitochondria and quantified as a ratio of TMRM positive events to Mitotracker-Green positive events (N=4). \**p* 0.05; \*\**p* 0.01; \*\*\**p* 0.001; \*\*\*\**p* 0.0001. N represents the number of independent experiments. EM image analysis was performed in a semi-automated platform by researcher who was blinded to the treatment conditions.



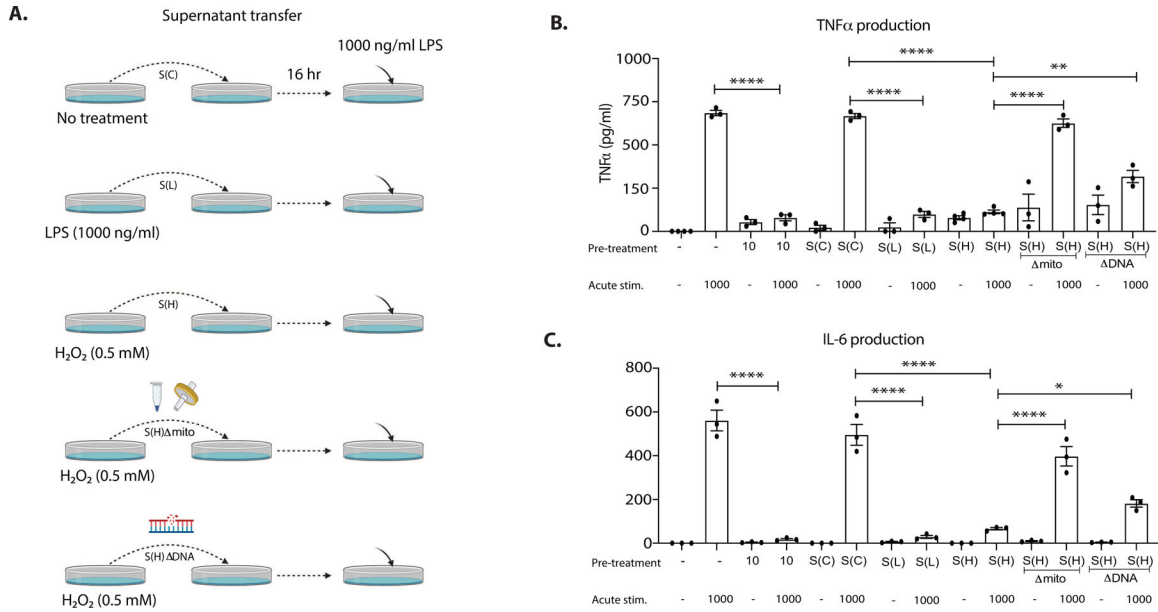


**Figure 5. Damaged extracellular mitochondria mediate endotoxin tolerance.**

(A) Schematic of supernatant transfer experiments: Cell supernatant was collected from healthy macrophages (S(C)), as well as macrophages which incurred mitochondrial damage by 1000 ng/ml LPS (S(L)) or 0.5 mM H<sub>2</sub>O<sub>2</sub> (S(H)). To characterize impact of extracellular mitochondria, the S(H) supernatant underwent filtration and high-speed centrifugation (S(H)- mito) for removal of intact mitochondria. Additionally, to characterize impact of extracellular mtDNA, the S(H) supernatant underwent DNAase digestion to remove mtDNA (S(H)- DNA). These different conditioned media were used to treat naïve macrophages for 16 hours before exposing them to high dose LPS (1000 ng/ml) for 6 hours. Pro-inflammatory cytokine production in response to high dose LPS treatment was evaluated by quantifying (B) TNFα (N=3) and (C) IL-6 levels (N=3) by ELISA. Analysis was performed using one-way ANOVA along with Tukey’s multiple comparisons between each treatment group. \*p < 0.05; \*\*p < 0.01; \*\*\*p < 0.001; \*\*\*\*p < 0.0001. N represents the number of independent experiments.